Recent changes in pan-Arctic melt onset from satellite passive microwave measurements

L. Wang,[1] C. Derksen,[1] R. Brown,[2] and T. Markus[3]

[1]   A new satellite passive microwave (PMW) melt onset retrieval algorithm based on temporal variations in the differences of the brightness temperature between 19 and 37 GHz is shown to be as effective as radar (e.g., QuikScat) measurements. The PMW technique shows improved melt estimates that are more closely linked to observed snow-off dates than previous studies. An integrated pan-Arctic (north of 50°N) melt onset date (MOD) dataset is produced by combining estimates on land and sea ice for the entire satellite PMW record. During the 1979–2011 period, significant trends of 2~3 days (decade)$^{-1}$ to earlier MOD are mainly concentrated over the Eurasian land sector of the Arctic, consistent with changes in spring snow cover extent observed with visible satellite data. The variability and change in melt onset are largely driven by spring surface air temperature, with insignificant influence from low-frequency modes of atmospheric circulation.
Citation: Wang, L., C. Derksen, R. Brown and T. Markus (2013), Recent changes in pan-Arctic melt onset from satellite passive microwave measurements, *Geophys. Res. Lett.*, *40*, 522–528, doi:10.1002/grl.50098.

1.   Introduction

[2]   The Arctic has experienced rapid warming and increasing winter precipitation in recent decades [*Trenberth et al.*, 2007; *Min et al.*, 2008]. Arctic snow cover has shown very different regional responses to these changes. For example, snow depth is increasing in many regions of Eurasia [EUR; *Bulygina et al.*, 2009], while widespread decreases in snow depth are evident in North America [NA; *Callaghan et al.*, 2011]. Based on the National Oceanic and Atmospheric Administration (NOAA) weekly snow chart dataset, the spring snow cover extent (SCE) has exhibited more negative trends in EUR than NA Arctic [*Brown et al.*, 2010; *Derksen and Brown*, 2012]. This contrasts with trends in spring snowmelt derived from satellite passive microwave (PMW) data that show more of a consistent pan-Arctic response [*Tedesco et al.*, 2009]. Surface air temperature (SAT) was found to exert the most significant influence on the inter-annual variability in spring SCE [*Brown et al.*, 2010; *Derksen and Brown*, 2012]. However, the seasonal strength of the Arctic Oscillation (AO) index was also found to significantly influence the inter-annual variability in melt onset date (MOD) on the Arctic sea ice and across the Eurasian terrestrial Arctic [*Drobot and Anderson*, 2001; *Belchansky et al.*, 2004; *Tedesco et al.*, 2009].

[3]   Microwave satellites are effective tools for examining changes in snow melt dynamics over the Arctic due to their high sensitivity to liquid water in snow and generally absence of the cloud cover issues faced by visible satellite imagery [*Wang et al.*, 2008; *Markus et al.*, 2009]. *Wang et al.* [2011] developed an integrated pan-Arctic melt onset dataset by combining active and passive microwave-derived estimates for the northern high-latitude land surface, ice caps, large lakes, and sea ice for the period 2000–2009. A major advantage of the integrated dataset is that it allows melt dynamics to be examined in a full pan-Arctic context and to explore interactions between the terrestrial and marine components of the cryosphere. The dataset also lends itself well to the evaluation of climate model simulations in the spring period when models exhibit significant spread in simulated snow cover [*Slater et al.*, 2001]. It also provides independent validation of trends in terrestrial snow cover extent observed with visible satellite dataset [e.g., *Derksen and Brown*, 2012] as satellite microwave-derived MOD estimates have been shown to be significantly correlated with observed snow-off dates [*Wang et al.*, 2008].

[4]   Compared to enhanced resolution active microwave QuikScat (QS) data (~5 km), the PMW data have a coarser resolution (25 km) and were previously found to be less sensitive to melt [*Ashcraft and Long*, 2006]. The QS data are only available from June 1999 to November 2009 when the antenna stopped working. The development of a new PMW melt detection technique is necessary to take advantage of a longer historical satellite record. Thus, the objectives of this study are as follows:

[5]   1. to present a new improved melt detection algorithm for PMW data capable of identifying multiple melt events and produce melt estimates closely correlated to the end of snow season (as developed for QS in *Wang et al.* [2008]);

[6]   2. to extend the 10 year pan-cryosphere integrated melt dataset of *Wang et al.* [2011] to the whole satellite PMW data record;

[7]   3. to analyze trends in MOD over Arctic land and sea ice and examine the relative roles of warming and atmospheric circulation in the observed variability and change in MOD over the period 1979–2011.

[1]Climate Research Division, Atmospheric Science and Technology Directorate, Environment Canada, Toronto, Ontario, Canada.
[2]Climate Research Division, Ouranos, Environment Canada, Montreal, Quebec, Canada.
[3]Cryospheric Sciences Branch, NASA Goddard Space Flight Center, Greenbelt, Maryland, USA.

Corresponding author: L. Wang, Climate Research Division, Atmospheric Science and Technology Directorate, Environment Canada, 4905 Dufferin St. Toronto, ON M3H 5T4, Canada. (Libo.Wang@ec.gc.ca)

2.   Data and Methods

[8]   This study uses daily brightness temperatures (Tbs) from the scanning multichannel microwave radiometer

Table 1. Data Periods for the Different Satellite Passive Microwave Radiometers and Overpass Used for Melt Detection in This Study

| Satellite	Start Date	End Date	Overpass
Nimbus-7 SMMR	Oct 1978	Aug 1987	Ascending
F-08 SSM/I	Jul 1987	Dec 1991	Descending
F-11 SSM/I	Dec 1991	May 1995	Ascending
F-13 SSM/I	May 1995	Apr 2009	Ascending
F-17 SSMIS	Dec 2006	Present	Ascending

(SMMR, 1979–1987), the special sensor microwave/imager (SSM/I, 1987–2008), and the special sensor microwave imager/sounder (SSMIS, 2009 to present) mapped to 25 km EASE-Grid available from the National Snow and Ice Data Center in Boulder, Colorado [*Armstrong et al.*, 1994; *Knowles et al.*, 2002]. These sensors provide a continuous time series of Tb since 1979 (Table 1). Sensor cross calibration is performed following *Jezek et al.* [1993] for the SMMR to SSM/I F-08, *Abdalati et al.* [1995] for the F-11 to F-08, and *Stroeve et al.* [1998] for F-13 to F-11, which is the same methodology used by *Markus et al.* [2009] for melt detection on sea ice. We do not perform calibration from SSMIS F-17 to SSM/I F-13 (consistent with *Cavalieri et al.* [2012]). Since our melt detection algorithm (described below) only uses the relative change in the temporal variations in Tb, slight offsets in Tbs between sensors should not affect algorithm performance. The gaps in the data are filled by linear interpolation from adjacent days. Vertically polarized Tbs from afternoon orbits are used for melt detection in this study (Table 1). The overpass time for the SSM/I(S) sensors have an equatorial crossing time near 1800 for the afternoon orbits, while the ascending equatorial crossing time for SMMR is near 1200. We believe that the inter-sensor calibration should have minimized the difference in Tbs due to different crossing times between SMMR and SSM/I(S) sensors. Nevertheless, the differences

in the SMMR and SSM/I(S) sensors may still introduce some uncertainties in the long-term trends of MOD (as explained in *Tedesco et al.* [2009], this uncertainty cannot be quantified).

[9] As in *Wang et al.* [2008], daily air temperature and snow depth observations from the World Meteorological Organization (WMO, http://www.ncdc.noaa.gov) weather stations archived at the National Climate Data Center were used for melt detection algorithm development and evaluation. Since the microwave response of melt on permanent snow and ice is different from seasonal terrestrial snow cover, we mask out the Greenland ice sheet and glaciers in our analyses.

[10] The channel difference between 19 GHz (SSM/I(S)) or 18 GHz (SMMR) and 37 GHz from the PMW sensors has been used to detect terrestrial snowmelt in the northern high latitudes [e.g., *Takala et al.*, 2009]. Time series of the differences in Tb (TbD = 19V-37 V) exhibit very similar characteristics as time series of backscatter (σ°) from QS in terms of melt detection (Figure 1). Using Figure 1 as an example, when SAT approaches 0°C at day of year (DOY) 109 and 128, there are apparent decreases around these dates in both TbD and σ°. They both return to their respective winter pre-melt values following the drop of SAT to below freezing. The final ablation of the snowpack starts at DOY 134, and the surface is snow free at DOY 152 according to observations at the station (Figure 1b). There are large decreases in both TbD and σ° at DOY 134, and they approach their respective snow-free summer values after DOY 152 (Figure 1a).

[11] *Wang et al.* [2008] developed an algorithm capable of distinguishing preliminary melt events from the main melt event using QS data. In this study, we develop a similar algorithm for melt detection from time series of PMW TbD. MOD is detected if the difference in daily TbD and the previous 3-day average (M) is greater than a threshold (TH1 = 0.35*M) for four or more consecutive days. Since TbDs
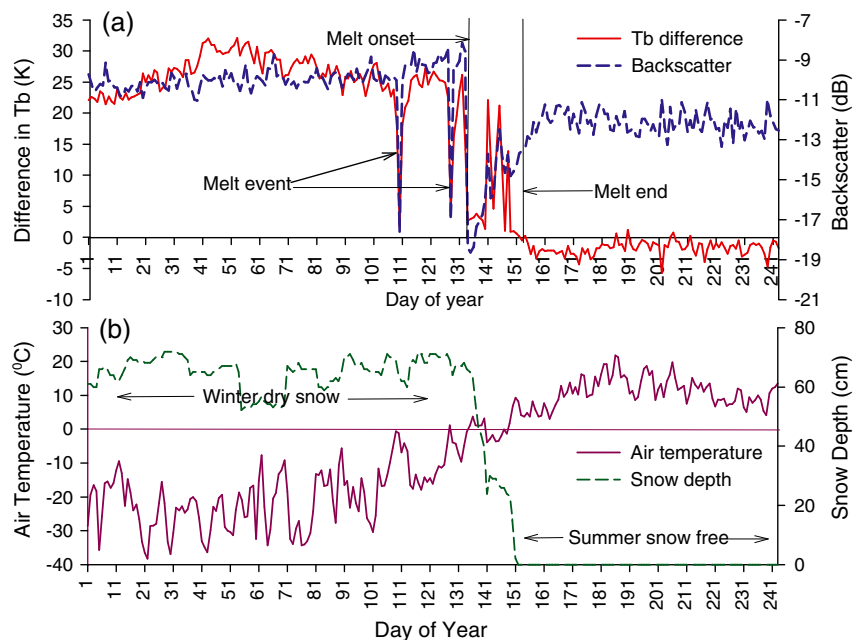
Figure 1. (a) Example time series of QS backscatter (dB) and SSM/I Tb difference (K) and (b) Daily surface air temperature (°C) and snow depth (cm) at Dudinka station (69.4°N, 86.167°E) in 2005.
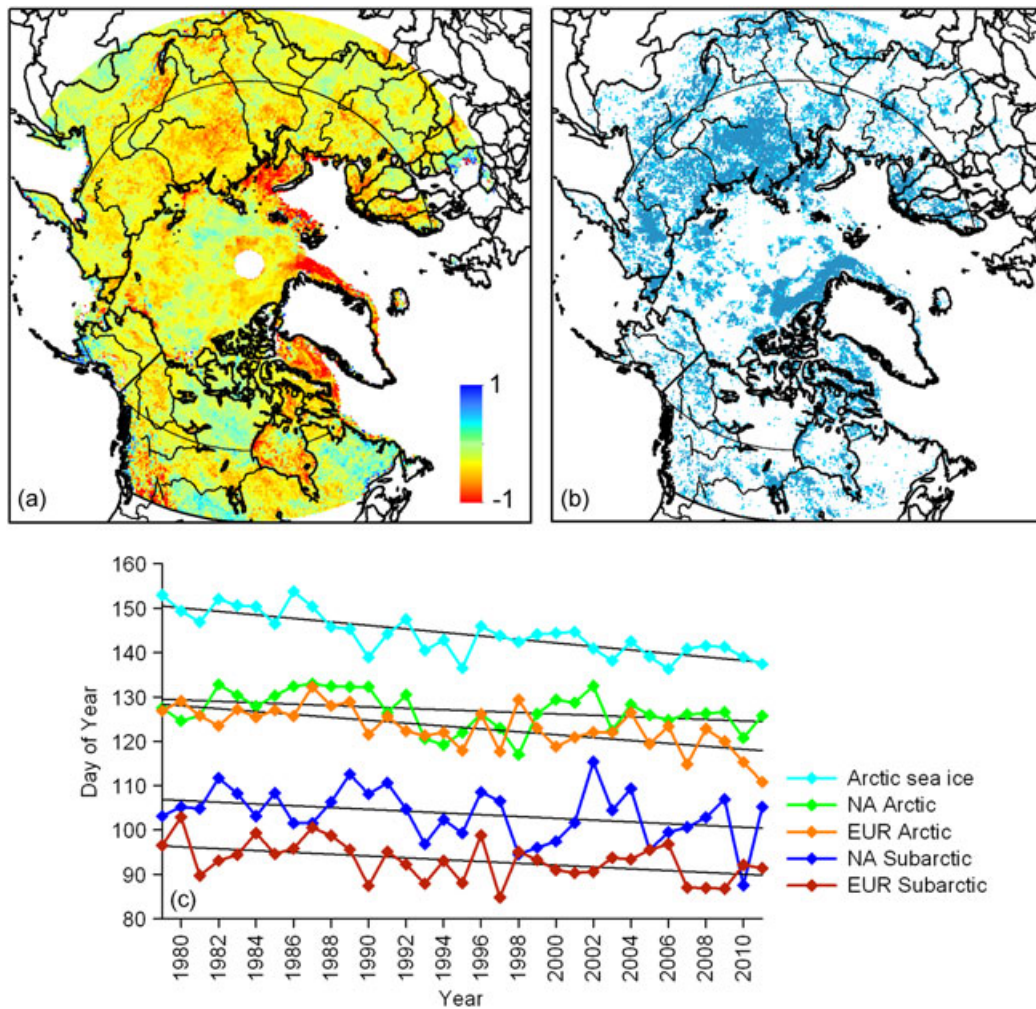
Figure 2. (a) Linear least squares trends (days/year), (b) the associated P values for local significance over the 1979–2011 period, and (c) time series of latitudinally averaged MOD in the Subarctic and Arctic zones of NA and EUR. Trend estimates were computed from least squares and are summarized in Table 2.

have similar magnitudes for the melting days and for the snow-free summer period, we cannot adopt a similar approach as in *Wang et al.* [2008] for melt end date (MED) detection. Instead, we establish an iterative approach for MED detection from PMW: melt end is detected as the first day when daily TbD is less than a threshold (TH2) for at least 28 days continuously. If these conditions are not met at a certain grid cell, we reduce the number of days to 21, and then to 14 if necessary. By trial and error, we found that

TH2 = average TbD in July plus 7 K gave the best results when compared to observations. Following *Takala et al.* [2009], we compared the histograms of the differences in MED from PMW and snow-off dates from WMO stations for SMMR years (1980–1987) and SSM/I years (2000–2007). While relatively poor correlations ($r^2 = 0.4$) were found in a previous study [*Tedesco et al.*, 2009], our results show that MED and snow-off are closely correlated, with $r^2 = 0.72$ and $r^2 = 0.68$ for the SMMR and SSM/I

Table 2. Least Squares Trends in Latitudinally Averaged MOD (days/year) and Spring SAT (°C/year) During 1979–2011[a]

	Subarctic					Arctic				
	MOD (days/year)	SAT (°C/year)				MOD (days/year)	SAT (°C/year)			
		March	April	May	MAM		April	May	June	AMJ
NA	−0.20	−0.036	0.009	−0.002	−0.010	−0.16	0.057	0.036	**0.035**	**0.043**
		% congruent with SAT			19.8		% congruent with SAT			80.9
EUR	**−0.21**	0.064	**0.064**	**0.031**	**0.053**	**−0.33**	**0.081**	**0.048**	0.037	**0.055**
		% congruent with SAT			90.6		% congruent with SAT			77.2
Sea ice						**−0.40**	**0.128**	**0.067**	0.014	**0.070**
							% congruent with SAT			71.8

[a]Bold values represent significant trends at 95% level. Also shown is the fraction (%) of seasonally averaged MOD trends congruent with trends in SAT. SAT for land regions (NA and EUR) is from the CRU dataset, and SAT is from the ERA-Interim for the sea ice region.
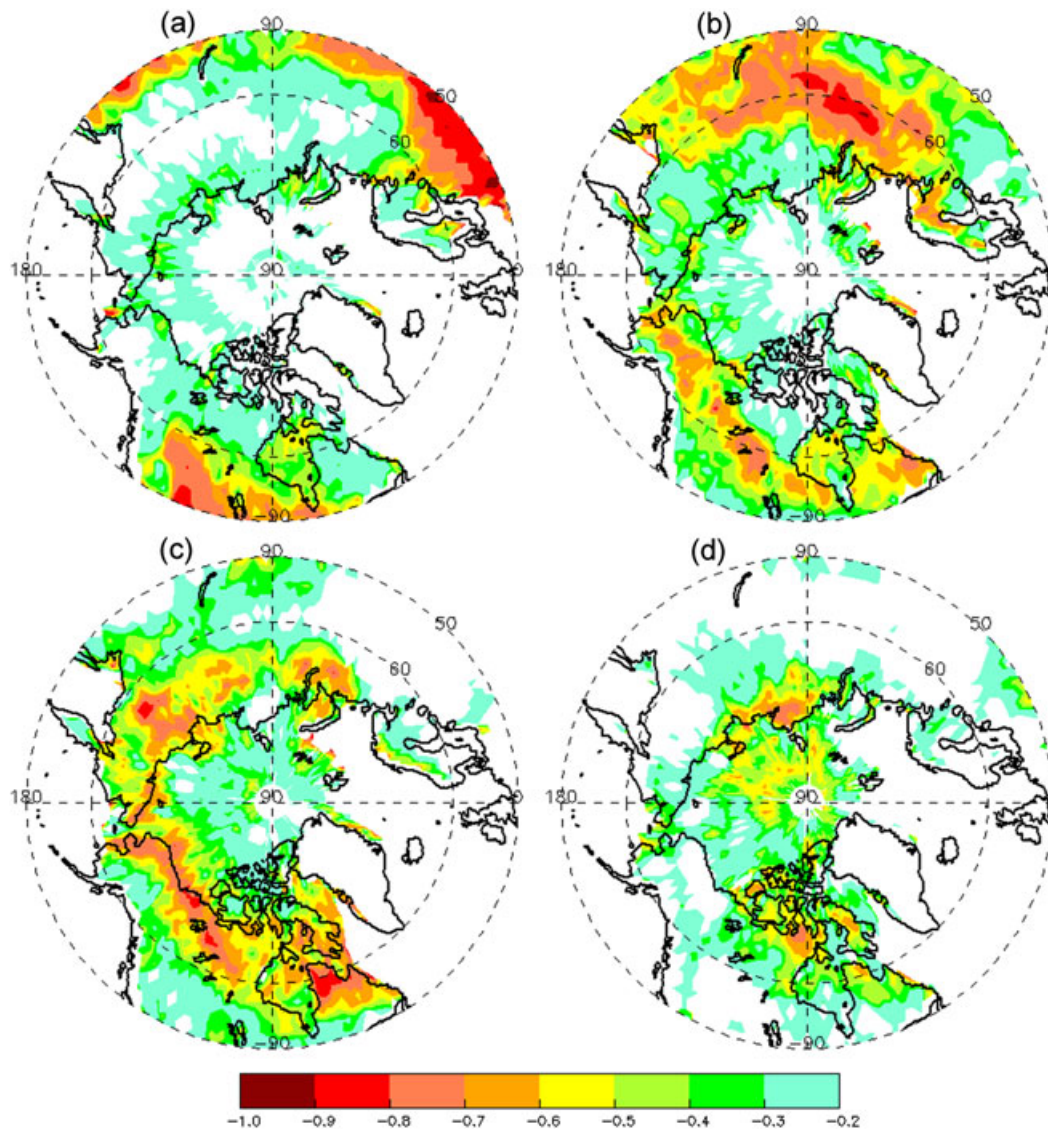
Figure 3. Correlations of MOD and the ERA-Interim SAT in (a) March, (b) April, (c) May, and (d) June over the period 1979–2011. Correlations less than −0.3 are statistically significant at 95% confidence level.

years, respectively. The similar results in the histograms (see Figure S1 in the Supporting Information) indicate that our approach for MED detection performs consistently for the SMMR and the SSM/I sensors. Melt duration is the number of days between MOD and MED for each melt event. As in *Wang et al.* [2008], the main melt event is identified as the event with the longest melt duration. MODs associated with the main melt events are produced each year for land areas north of 50°N where there is relatively stable snow accumulation each winter.

[12] Following *Wang et al.* [2011], we produce an integrated MOD dataset by combining PMW estimates on land in this study and sea ice melt onset from *Markus et al.* [2009, updated to 2011] for each year during the period 1979–2011. The mean melt onset date (MMOD) and the standardized anomalies in MOD were computed for each year.

[13] Gridded (5° × 5°) SAT over land areas was obtained from the Climatic Research Unit CRUtem3v dataset [*Brohan et al.*, 2006] and used to create latitudinally

averaged SAT series. ERA-Interim reanalysis 2 m air temperature [*Dee et al.*, 2011] over land and sea ice was used to conduct spatial correlation analyses between SAT, MOD, and atmospheric circulation indices. Atmospheric circulation indices that have significant impact on the Arctic climate, such as the AO and the Pacific/North American pattern (PNA) were obtained from the NOAA Climate Prediction Center (http://www.cpc.noaa.gov/products).

[14] Trends in MOD and spring SAT were computed using the linear least squares method. Trends in MOD were computed on a per grid cell basis and on regionally averaged series for two latitudinal land zones: (1) 50°N to 60°N (hereafter "Subarctic" zone), and (2) continental land areas north of 60°N (hereafter "Arctic" zone) in each sector of the Arctic, and for a sea ice region north of 60°N. Linear correlations between the anomalies in MOD, the circulation indices, and SAT were computed to investigate their influences on the variability in spring melt onset. All correlations were performed using detrended series. The significance levels of the regressions and correlations were determined using a

Table 3. Correlations Between Anomalies in MOD, Spring SAT (MAM for Subarctic, AMJ for Arctic), AO, and PNA During 1979–2011[a]

	Subarctic			Arctic		
Region	SAT	AO	PNA	SAT	AO	PNA
NA	**−0.78**	**0.43**	**−0.60**	**−0.62**	0.23	**−0.33**
EUR	**−0.72**	**−0.56**	**0.32**	**−0.70**	−0.27	0.19
Sea ice				**−0.72**	**−0.36**	0.07

[a]Bold values represent significant correlations at 95% level. SAT for land regions (NA and EUR) is from the CRU dataset, and SAT is from the ERA-Interim for the sea ice region.

two-tailed Student's *t* test. All reported correlations are statistically significant at a significance level of 0.05.

[15] To evaluate the contribution of warming trends versus atmospheric circulation indices on the melt onset trends, we compute the component of the trends that is linearly congruent with the other factor (X) as in *Thompson et al.* [2000]. First, we regress time series of MOD onto X, then multiply the resulting regression coefficient by the ratio of the trend in X and MOD.

3. Results

[16] Following *Tedesco et al.* [2009], we compared MOD derived from PMW in this study to those derived from QS using the method of *Wang et al.* [2008] for the 2000–2009 period (Figure S2). The results show that the differences between the two datasets are within ±4 days for 72% of Arctic areas, with relatively larger differences (<10 days) only in limited areas with either dense forest or high relief that pose challenges for both QS and PMW melt detection [*Wang et al.*, 2008]. Applying a *t* test for difference in means shows that about 10% of the pan-Arctic region has significant differences (p < 0.05) between the two datasets, mainly located in mountainous western NA. For some dense forest and high-relief areas, melt is not detected from QS, while melt

is resolved from the PMW algorithm (an example is shown in Figure S3). This is because the range for TbD from dry snow to melting snow is about 30 K (Figure 1), much larger than that for σ° (~10 dB), which makes it more effective for melt detection in dense forest areas where the melt signal is diminished [*Wang et al.*, 2008].

[17] Most of the Arctic sea ice and land areas exhibit negative (earlier melt onset) trends during the 1979–2011 period (Figure 2a). However, locally significant negative trends are mainly concentrated in central and east Siberia and Scandinavia, and a narrow band on sea ice between the Northern Ellesmere Island/Greenland and the North Pole (Figure 2b). The latitudinally averaged MOD trends are not significant for either the Subarctic (−0.20 d yr^{-1}) or the Arctic (−0.16 d yr^{-1}) zones of NA (Table 2 and Figure 2c). Trends are significant in the EUR Arctic, with trends being more negative in the Arctic zone (−0.33 d yr^{-1}) than the Subarctic zone (−0.21 d yr^{-1}). This is consistent with the findings in *Dèry and Brown* [2007] of enhanced snow-albedo feedback at higher latitudes. For the Arctic zone, trends in EUR are more negative than those in NA, which are consistent with changes in spring SCE [*Brown et al.*, 2010; *Derksen and Brown*, 2012]. The regional MOD trends are more negative over the Arctic sea ice (−0.40 d yr^{-1}) than land (Table 2).

[18] Correlation analyses show that the inter-annual variability in MOD is significantly correlated with spring SAT (Figure 3 and Table 3). The area with significant temperature correlation moves northward during the melt season and is mainly confined to land areas (Figure 3). The weaker correlations over sea ice are considered to be related to ice dynamics [*Markus et al.*, 2009; *Maksimovich and Vihma*, 2012] and the rapid advancement of MOD over the central Arctic sea ice [*Wang et al.*, 2011] that is not captured at a monthly time scale. The negative correlations between JFM AO (average in January-February-March) and FMA PNA (average from February-March-April) and MOD are consistent with the correlations between spring SAT and
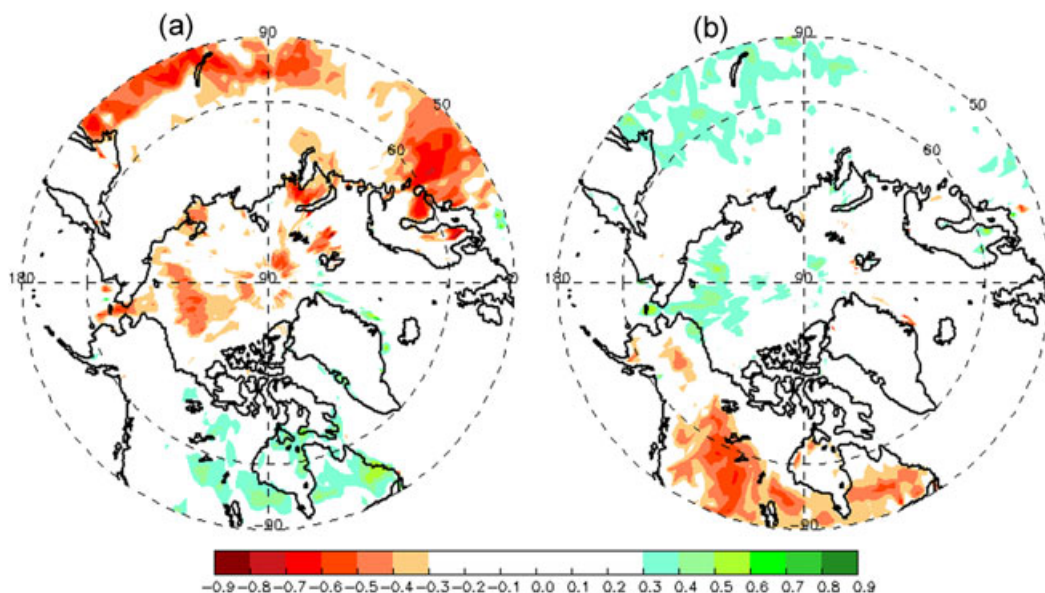
Figure 4. Correlations of MOD with (a) Jan.–Mar. AO and (b) Feb.–Apr. PNA over 1979–2011. Only locally statistically significant correlations at 95% confidence level are shown.

AO/PNA (Figure 4 and Figure S4). In general, a positive AO index is associated with warm SAT anomalies across EUR and cold SAT anomalies in eastern Canada. A positive PNA is associated with warm SAT anomalies in the middle to high latitudes of western NA.

[19] During recent years, the AO and PNA indices are more variable, and trends in the JFM AO (0.008/year) or FMA PNA (−0.008/year) are weak and not significant over the 1979–2011 period. Trends in JFM AO and FMA PNA only contribute small fractions (10%–30%) to trends in MOD during the 1979–2011 period (Figure S5). Regional trends in MOD and spring SAT (Table 2) show that significant trends to earlier MOD occurred over the two latitudinal land zones in EUR and for Arctic sea ice, consistent with significant warming over the melt season. The lack of significant trends in MOD over NA is consistent with the SAT trends that show no evidence of significant warming over the spring period. Analysis of the contribution of SAT to MOD trends showed that temperature accounts for 77%–91% of the trend in MOD except for the NA Subarctic (~20%).

4. Discussion and Conclusions

[20] In this study, we develop an algorithm capable of separating multiple early melt events from the main melt event using satellite PMW measurements. The new algorithm shows improved melt estimates that are more closely linked to observed snow-off dates than a previous pan-Arctic study [*Tedesco et al.*, 2009]. The TbD from the 19 and 37 GHz PMW measurements proves to be as effective as $\sigma°$ from QS for multiple melt event detection. On account of the large range in TbD, the PMW algorithm performs better in dense forest and high-relief areas than QS data even though the spatial resolution is coarser. The correlation between MED and snow-off in this study is not as strong as that found by *Wang et al.* [2008] from QS estimates. One of the main reasons is because the end date of melting snow cannot be identified directly from TbD (see section 2), while $\sigma°$ from QS can explicitly detect melt end [*Wang et al.*, 2008].

[21] The spatial pan-Arctic MOD trends from PMW data in this study are consistent with PMW-derived results for Arctic sea ice [*Maksimovich and Vihma*, 2012] and the Northern Hemisphere land surface [*Kim et al.*, 2012] with mostly non-significant trends except over a narrow band on central Arctic sea ice and land areas of Eurasia. *Kim et al.* [2012] suggest that the lack of significant trends may be related to the large inter-annual variability in MOD. A previous study [*Tedesco et al.*, 2009] has documented pan-Arctic trends toward earlier MOD, but our results indicate greater spatial variability with the strongest trends toward earlier MOD over the Eurasian land sector of the Arctic, consistent with SCE trends from visible satellite data reported in *Derksen and Brown* [2012].

[22] *Tedesco et al.* [2009] found that up to 50% of the variance in MOD in EUR can be explained by the seasonal strength of the AO index during 1979–2008. Our study shows that for the period 1979–2011, the AO index is only significantly correlated with MOD in the Subarctic zone of NA and EUR. The PNA index has a relatively stronger influence on the variability in MOD in the Subarctic of NA. Compared to the influence of the AO and the PNA indices, the spring SAT has a much stronger influence on the variability in MOD in both sectors of the Arctic (Table 3),

consistent with findings in previous studies for spring SCE [*Brown et al.*, 2010; *Derksen and Brown*, 2012]. During the period 1979–2011, MOD trends are largely driven by changes in spring SAT, with only a small contribution characterized by the atmospheric circulation indices. Given the close link between MOD and SAT, continued monitoring of the variability and change in spring MOD from satellite will provide useful information on the response of the cryosphere to amplified warming in the Arctic.

References

Abdalati, W., K. Steffen, C. Otto, and K. C. Jezek (1995), Comparison of brightness temperatures from SSM/I instruments on the DMSP F8 and F11 satellites for Antarctica and the Greenland ice sheet, *Int. J. Remote Sens.*, 16, 1223–1229, doi:10.1080/01431169508954473.

Armstrong, R. L., K. W. Knowles, M. J. Brodzik and M. A. Hardman (1994), updated current year, DMSP SSM/I-SSMIS Pathfinder Daily EASE-Grid Brightness Temperatures, [list dates of data used], National Snow and Ice Data Center. Digital media, Boulder, CO.

Ashcraft, I. S., and D. G. Long (2006), Comparison of methods for melt detection over Greenland using active and passive microwave measurements, *Int. J. Remote Sens.*, 27, 2469–2488.

Belchansky, G. I., D. C. Douglas, and N. G. Platonov (2004), Duration of the Arctic sea ice melt season: Regional and interannual variability, 1979–2001, *J. Clim.*, 17, 67–80.

Brohan, P., J. J. Kennedy, I. Harris, S. F. B. Tett, and P. D. Jones (2006), Uncertainty estimates in regional and global observed temperature changes: A new data set from 1850, *J. Geophys. Res.*, 111, D12106, doi:10.1029/2005JD006548.

Brown, R., C. Derksen, and L. Wang (2010), A multi-dataset analysis of variability and change in Arctic spring snow cover extent, 1967–2008, *J. Geophys. Res.*, 115, D16111, doi:10.1029/2010JD013975.

Bulygina, O. N., V. N. Razuvaev, and N. N. Korshunova (2009), Changes in snow cover over Northern Eurasia in the last few decades. *Environ. Res. Lett.*, 4, 045026, doi:10.1088/1748-9326/4/4/045026.

Callaghan, T., et al. (2011), The changing face of Arctic snow cover: A synthesis of observed and projected changes, *Ambio*, 40, 17–31.

Cavalieri, D. J., C. Parkinson, N. DiGirolamo, A. Ivanoff (2012), Intersensor Calibration Between F13 SSMI and F17 SSMIS for Global Sea Ice Data Records, NASA technical report, 13 pp.

Dee, D. P., et al. (2011), The ERA-Interim reanalysis: Configuration and performance of the data assimilation system, *Q J Roy Meteor Soc.*, 137, 553–597, doi: 10.1002/qj.828.

Derksen, C., and R. Brown (2012), Spring snow cover extent reductions in the 2008–2012 period exceeding climate model projections, *Geophys. Res. Lett.*, 39, L19504, doi:10.1029/2012GL053387.

Dèry, S. J., and R. D. Brown (2007), Recent Northern Hemisphere snow cover extent trends and implications for the snow-albedo feedback, *Geophys. Res. Lett.*, 34, L22504, doi:10.1029/2007GL031474.

Drobot, S. D., and M. R. Anderson (2001), Comparison of interannual snowmelt-onset dates with atmospheric conditions, *Ann. Glaciol.*, 33, 79–84.

Jezek, K. C., C. J. Merry, and D. J. Cavalieri (1993), Comparison of SMMR and SSM/I passive microwave data collected over Antarctica, *Ann. Glaciol.*, 17, 131–136.

Kim, Y., J. S. Kimball, K. Zhang, K. C. McDonald (2012), Satellite detection of increasing Northern Hemisphere non-frozen seasons from 1979 to 2008: Implications for regional vegetation growth, *Rem. Sens. Environ.*, 121, 472–487.

Knowles, K. W., E. G. Njoku, R. L. Armstrong, and M. J. Brodzik. 2002. Nimbus-7 SMMR Pathfinder Daily EASE-Grid Brightness Temperatures, National Snow and Ice Data Center. Digital media, Boulder, CO.

Maksimovich, E., and T. Vihma (2012), The effect of surface heat fluxes on interannual variability in the spring onset of snow melt in the central Arctic Ocean, *J. Geophys. Res.*, 117, doi:10.1029/2011JC007220.

Markus, T., J. C. Stroeve, and J. Miller (2009), Recent changes in Arctic sea ice melt onset, freeze-up, and melt season length, *J. Geophys. Res.*, 114, C12024, doi:10.1029/2009JC005436.

Min, S. K., X. B. Zhang, and F. Zwiers (2008), Human-induced arctic moistening. *Science*, 320, 518–520.

Slater, A. G., C. A. Schlosser, C. E. Desborough, A. J. Pitman, A. Henderson-sellers, A. Robock, et al. (2001), The representation of snow in land surface schemes: Results from PILPS 2(D). *J. Hydrometeor.*, *2*, 7–25.

Stroeve, J., J. Maslanik, and L. Xiaoming (1998), An intercomparison of DMSP F11- and F13-derived sea ice products, *Remote Sens. Environ.*, *64*, 132–152, doi:10.1016/S0034-4257(97)00174-0.

Takala, M., J. Pulliainen, S. J. Metsamaki, and J. Koskinen (2009), Detection of snowmelt using spaceborne microwave radiometer data in Eurasia from 1979 to 2007, *IEEE Trans. Geosci. Rem. Sens.*, *47*, 2996–3007.

Tedesco, M., M. Brodzik, R. Armstrong, M. Savoie, and J. Ramage (2009), Pan arctic terrestrial snowmelt trends (1979–2008) from spaceborne passive microwave data and correlation with the Arctic Oscillation, *Geophys. Res. Lett.*, *36*, L21402, doi:10.1029/2009GL039672.

Thompson, D. W. J., J. M. Wallace, and G. Hegerl (2000), Annular modes in the extratropical circulation. Part II: Trends, *J. Clim.*, *13*, 1018–1036.

Trenberth, K. E., et al. (2007), Observations: surface and atmospheric climate change, in Climate Change 2007: The physical science basis, Cambridge University Press, Cambridge, United Kingdom and New York, NY, USA.

Wang, L., G. Wolken, M. Sharp, S. Howell, C. Derksen, R. Brown, T. Markus, and J. Cole (2011), Integrated pan-Arctic melt onset detection from satellite active/passive microwave measurements, 2000–2009, *J. Geophys. Res.*, doi:10.1029/2011JD016256.

Wang, L., C. Derksen, and R. Brown (2008), Detection of pan-Arctic terrestrial snowmelt from QuikSCAT, 2000–2005, *Rem. Sens. Environ.*, *112*, 3794–3805.